



Temporal Dynamics of Tree Crown Fractal Dimension in Two Species of Deciduous Oaks

Graciela Jiménez-Guzmán¹ · Ernesto Vicente Vega-Peña²

Accepted: 19 December 2023
© The Author(s) 2024

Abstract

Fractal dimension (D) can be used to characterise temporal changes of crown architecture of individual trees. Our goal in this study was to analyse seasonal changes in tree crown fractal dimension of two species of deciduous oaks (*Quercus castanea* and *Q. obtusata*) coexisting in a natural forest in central Mexico using low cost sampling, and relate these changes to morphological attributes and environmental variables.

Every two months, from May 2017 to September 2018, for each oak species, we photographed fixed portions of the crowns of individual trees, measured their trunk diameters, and obtained average temperature and accumulated precipitation data recorded for the sampling date. From the obtained images, we calculated D values by the semivariogram method using three different variability estimators (square increment, isotropic, and transect variation).

We identified a positive correlation between D and temperature, and a negative correlation between temperature and crown cover.

The fractal dimension (D) of crowns of two deciduous oak species changes according to the tree's phenological stage. D values varied through time in relation to tree crown phenological variation, but not with crown cover dimension. We propose a model of annual D value fluctuation in deciduous trees, characterised by two high complexity peaks and two low complexity valleys, corresponding to the effects on crown cover of annual periods of leaf abscission and development.

Keywords Fractal Dimension · Tree Phenology · Canopy · Oak

✉ Ernesto Vicente Vega-Peña
evega@iies.unam.mx

Graciela Jiménez-Guzmán
gjimenez@iies.unam.mx

¹ Posgrado en Ciencias Biológicas, Universidad Nacional Autónoma de México, Mexico City, Mexico

² Instituto de Investigaciones en Ecosistemas y Sustentabilidad, Universidad Nacional Autónoma de México, Morelia Michoacán, Mexico

Introduction

The form of the crown determines how trees make use of essential resources like light and carbon dioxide (Ishii & Asano 2010), which makes its study relevant because form is the product of each tree species' genetic adaptation (Bailey et al. 2004; Yang & Hwa 2008), their responses to stress (Oancea et al. 2017; Yang et al. 2015), and the surrounding environmental conditions (Pangga et al. 2013; MacLeod & Steart, 2015; Sala et al. 2020). Regarding the latter responses, the strong impact of climatic variables like temperature and precipitation on the growth and dynamics of tree crowns—especially of deciduous trees—was previously established (Ehbrecht et al. 2017; Sala et al. 2020). The seasonal variation of temperature and precipitation influences canopy dynamics in trees, impacting key physiological processes, like leaf production, photosynthesis, and carbon allocation. Warmer temperatures and greater water availability may accelerate these processes, affecting the duration of the growing season and overall leaf area. Another important aspect of crown phenology is its role on forest community structure. Non-overlapping phenological patterns can be a way for tree species to coexist in a forest (Ishii & Asano, 2010).

Because tree crowns grow following modular and iterative patterns, their study can assume them to be fractal objects (Seidel et al. 2019; Xu et al. 2020). Fractal objects are apparently irregular shapes for which Mandelbrot (1982) developed a theory for their analysis. One of the characteristics of fractal objects is that their attributes (like length or area) depend on the scale used for their measurement. For example, to calculate the area of a circumference (or any other regular shape) inscribed inside a square, we can divide the area into a grid to count the number of squares included within the circumference, the area progressively increasing as we reduce the size of the squares in the grid, until reaching a constant value. Instead, the area of a fractal object would continue to decrease indefinitely as the grid's squares become smaller (Hastings & Sugihara, 1993, p. 37). Within the context of Euclidean geometry, regular objects like lines, shapes, or volumes, are associated to a dimension that is expressed as a whole number (1, 2, or 3, respectively), but the dimension of fractal objects is expressed in real numbers. The fractal dimension (D) is a decimal describing the complexity of the shape (Bruno et al. 2008; Oancea et al. 2017; Seidel 2018). In the case of 2D images (photographs) taken from tridimensional objects (tree crowns), the D values will range between 2 and 3 and a fractal shape with $D \approx 2$ would be less complex than another one with $D \approx 3$ (Musarella et al. 2018; Nayak et al. 2019). Many natural objects and processes have attributes that can be considered as fractal. So, fractal theory and its methods offer a unified way for studying them and find their shared characteristics (Mandelbrot, 1982). Applications of fractal indexes in ecology are diverse, ranging from analyzing of cellular, protein and chromosome structure, DNA sequences and enzyme kinetics (Kenkel and Walker, 1996), to measuring habitat space, detecting functional hierarchies and assessing persistence of rare species (Sugihara and May, 1990).

Determining D values has been a challenge for which several mathematical methods have been developed, as reviewed by Nayak et al. (2019) for complex natural objects, and by Arseniou and MacFarlane (2021) for tree crowns. In the context of tree architecture, authors like Zeide and Pfeifer (1991), Osawa (1995), Foroutan-pour

et al. (2000), Zhu et al. (2014), Dutilleul et al. (2015), Zhang et al. (2011), Arseniou and MacFarlane (2021), among others, used D to describe the fractal complexity of plants and tree crowns, proposing multiple approaches for the calculation of fractal shapes. In this study, we considered using 2D shapes (photographs) because they facilitate the calculation of D values and are easy to interpret (Pentland 1984; Zhang et al. 2011; Ivošević et al. 2015; Ivošević et al. 2017). The estimation of D values does not replace the measurements traditionally used in plant studies like cover, but can be considered as a complementary attribute (Backhaus & Nehl 1999).

In previous studies, Foroutan-pour et al. (2000), Arseniou and MacFarlane (2021) and Seidel (2018) established that the complexity of individual plant canopies estimated by D values behaves dynamically in direct proportion to their growth stage and size. In this work, to explore the possible effect on crown geometric complexity of phenology in two deciduous species of oak (*Quercus castanea* and *Q. obtusata*), we set the goal of analysing annual changes in crown fractal dimension of trees from both oak species coexisting in a natural forest in central Mexico and relating these changes to morphological attributes, season, and weather variables. Warmer temperatures and greater water availability will stimulate leaf production and therefore increase biomass in the crown. Such changes in crown attributes will be reflected in its fractal dimension. Also it is expected that phenological patterns of the two species differ, suggesting a coexistence strategy. For that, we designed a non-invasive, low cost, sampling methodology.

Materials and Methods

Study Site and Studied Species

The study site is located in the Tsintani Renacer Voluntarily Conservation Area—certified by the Secretariat of Environment and Natural Resources of Mexico (SEMARNAT) for the 2013–2033 period—(19°28'22" N 101°21'38" W) in the municipality of Acuitzio del Canje, Michoacán, Mexico. The vegetation in the study site is of mixed pine-oak forest and the climate is temperate with summer rain (Cb(w2) (w) (i') g) (García, 1964). Total annual accumulated rain is around 1000 mm, with a monthly average of 83.6 mm (CV=86.25%). The highest mean monthly temperature is recorded in May (18 °C), and the summer months (June–September) have the highest precipitation of up to 200 mm per month (Carlón & Mendoza, 2007).

The species chosen for the study were *Quercus castanea* Née (Family Fagaceae, Section Lobatae Loudon) and *Q. obtusata* Bonpl. (Section *Quercus*), which are the most abundant trees in the study site, are deciduous, and grow at elevations between 1,400 and 2,800 m a.s.l. (Romero-Rangel et al. 2014).

Sampling

Samplings were made bimonthly between May 2017 and September 2018 to record tree parameters and establish the heterogeneity of the dry and wet seasons (Table 1). Morphological attributes and thus physiology of deciduous trees change during a

Table 1 Sampling dates, seasons, and corresponding mean monthly temperature and accumulated precipitation of each interval

Sampling ID	Sampling date	Days	Julian date	Julian date sampling ID	Season [†]	Mean temperature (°C)	Accumulated precipitation (mm)
1	May 9, 2017	0	129	3	Dry (Spring)	20.98	0.25
2	July 3, 2017	55	184	5	Rainy (Summer)	22.49	12.69
3	September 5, 2017	119	248	6	Rainy (Summer)	20.52	17.2
4	November 14, 2017	189	318	8	Dry (Fall)	19.34	4.67
5	January 23, 2018	259	23	1	Dry (Winter)	15.61	0
6	March 14, 2018	309	73	2	Dry (Winter)	18.36	0.95
7	May 24, 2018	380	144	4	Dry (Spring)	21.21	4.96
8	September 24, 2018	503	267	2	Rainy (Fall)	19.5	12.077

NOTE: [†]Dry: Accumulated rain in the period ≤ 5 mm. Rainy: Accumulated rain in the period > 5 mm. Source: Mean temperature and accumulated precipitation records for the sampling dates were obtained online from the monthly weather report of the Morelia weather station (Dirección de Medio Ambiente y Sustentabilidad, 2018)

year, mainly due to the season influence. In broad terms, there are four main phases recognized in the annual cyclic dynamics of crowns: foliation, stasis at maximum cover, defoliation, stasis without leaves (Bréda, & Granier 1996; Öztürk 2016).

To avoid measurements of individuals having crowns that overlapped other individual trees, single stem trees with at least one main branch not overlapping other tree crowns were chosen, and photographs of the non-overlapping crown zones were taken as described below. Another criterion used for branches selection was their cover sizes, which varied between 20 and 25% of total crown size. Thus we could be confident that branch phenology was a good proxy for the complete crown.

The dates of the measurements were recorded in the standard (dd/mm/yy) and Julian formats, the latter identifying dates as the number of days elapsed since January 1 of the corresponding year.

Design of the Non-Invasive Method for Capturing Tree Crown Images

Photographs were taken using a commercial 12.4 megapixel camera. The photographed percentages of tree crowns ranged between 30 and 100%. 10 photographs of the tree crown of each individual tree were always taken from the same point (Online Resource 1). A total of 4,400 colour photographs in.JPG format were taken. Afterwards, the 10 photographs for each tree crown for each sampling date were processed to obtain 440 black and white composite images (web appendix A), one for each tree and sampling date, from which the cover and D values were calculated as described below.

Data Processing

Estimation of D Values

For each composite image, crown D values were estimated using the `fractaldim.estim` function in the `fractaldim` package for R (Constantine & Percival 2014) of the statistical software R (R Core Team 2020). Because the images are binary matrices (that is, black and white images in which each pixel can have a value of either one or zero), the 2-dimensional calculation method was used. The D values were obtained using the variogram method, which begins calculating the semivariance $\gamma_{(h)}$ quantifying the variation of a set of X data at a spatial scale h , that is, the distance between data set elements:

$$\gamma_{(h)} = \frac{1}{2n_{(h)}} \sum_{i=1}^{n_{(h)}} [x_{(i)} - x_{(i+h)}]^2$$

where h is the distance between points (scale), $n_{(h)}$ is the total number of data for the h interval, $x_{(i)}$ is the value of the i th point, and $x_{(i+h)}$ is the value of the $i+h$ point (Palmer 1988). The h vs. $\gamma_{(h)}$ plot is the semivariogram. The D value of X can be obtained from the $\log(h)$ vs. $\log(\gamma_{(h)})$ plot, in which the slope of the regression m is included in $D=2- (m / 2)$ (Burrough 1981, Palmer 1988). In this work, the D of Gneiting et al. (2012) expression was used, which incorporates an estimation of the value of data variance (v_p):

$$D = 2 - \frac{1}{p} \left\{ \sum_{h \in K} \left(s_h - \bar{s} \right) \times \log \log v_p \left(\frac{h}{n} \right) \right\} \times \left\{ \sum_{h \in K} (s_h - \bar{s})^2 \right\}^{-1}$$

where K is the set of scales h , $s_h = \log(h/n)$ is the logarithm of the average distance between points at the h scale, n is the number of data in the h scale, \bar{s} is the average of s_h , and v_p is the variation estimator for the power index p , corresponding to the power index in $\gamma_{(h)}$, which for this study was $p=2$, because D is calculated for a surface. The smallest window size was used (argument `window.size=3` in the ‘`fd.estim`’ function) for obtaining the highest accuracy. The variation (v_p) was obtained following the square, isotropic and transect variation methods (Table 2).

Table 2 Variability estimators for the calculation of D following Gneiting et al. (2012)

NOTE: h : spatial scale. $n_{(h)}$: number of data in scale h ; $x_{(i)}$: value of the i -th point. l : number of lines in the surface. p : power index in $\gamma_{(h)}$ ($p=2$)

	Variability estimator	Variation equation [†]
D_s	square interval method:	$v_{S;p} \left(\frac{h}{n} \right) = \frac{1}{2n_{(h)}} \sum s_{(h)}$
D_i	isotropic method:	$v_{ISO;p} \left(\frac{h}{n} \right) = \frac{1}{2n_{(h)}} \sum s_{(h)}$
D_t	transect variation method:	$v_{TV;p} \left(\frac{l}{h} \right) = \frac{1}{2(n-2l)} \sum s_{(h)}$

Estimation of Crown Cover

Each pixel in the generated composite images had a value of 1 or 0, the values of 1 corresponding to zones in the image covered by tree crown and 0 to void zones. Therefore, the cover of the tree crowns was calculated as the sum of the pixels having a value of 1. Because the images captured different percentages of the crown (see Sect. 3), percentages of cover were calculated for each image. The maximum cover of each tree was calculated only considering the first seven samplings (corresponding to one year). Within the sampling period expressed in Julian days (days 0 to 380), the images showing the largest biomass for each tree were chosen and used as a reference of 100% crown cover. To obtain crown cover percentages for each sampling date (C), the expression $C = (PB_n \times 100) \times (PB_m)^{-1}$ was applied, where PB_n is the number of pixels with biomass in the image taken during the n sampling date, and PB_m is the maximum number of pixels calculated in the sampling date showing the largest biomass for the sampling period.

Estimation of Tree Size

The size of trees was estimated from crown diameter, height, and stem circumference at breast height measurements, estimating the basal area for each sampling date (Online Resource 2). The above-mentioned variables were analysed for group formation using linear discriminant analysis with a priori grouping of sampling dates; however, the results (not shown) were not statistically different. Nevertheless, the basal area (BA) values were used as a descriptor of individual tree size.

Estimation of Weather Variables

The accumulated precipitation (mm) and mean monthly temperature (°C) for each sampling period were used as weather variables, in the first sampling date using the records for the previous 60 days, and in subsequent samplings, the weather variables were calculated according to the number of days from the previous sampling date. The records of the chosen weather variables were obtained online from the monthly weather report of the Morelia weather station (Dirección de Medio Ambiente y Sustentabilidad, 2018) located 35 km from the study site (19°43'17" N 101°10'58" W), which is the nearest active weather station. During the studied period, the accumulated precipitation for each sampling period oscillated between 0 and 17.2 mm and the mean monthly temperature between 15.6 and 22.5 °C. The sampling date in which the highest precipitation values occurred corresponded to September, while the lowest values of precipitation and temperature were recorded in January (Table 1).

Statistical analyses

Relationships Between Weather Variables and Tree Architecture

The nonparametric Spearman correlation was used to identify possible relationships between tree morphometric attributes and weather variables. The analysed correlations between variables were: mean D_s -mean monthly temperature ($^{\circ}\text{C}$), mean D_s -accumulated precipitation (mm), mean D_i -mean monthly temperature ($^{\circ}\text{C}$), mean D_i -accumulated precipitation (mm), mean D_f -mean monthly temperature ($^{\circ}\text{C}$), mean D_f -accumulated precipitation (mm), mean C -mean monthly temperature ($^{\circ}\text{C}$), mean C -accumulated precipitation (mm), mean BA -mean monthly temperature ($^{\circ}\text{C}$), and mean BA -accumulated precipitation (mm). For each species, data from the eight sampling dates of the variables C - BA , D_s - C , D_s - BA , D_i - C , D_i - BA , D_f - C , and D_f - BA were analysed.

After, and because the weather variables data were averaged per sampling date, the mean values of D_s , D_i , D_f , C , and BA were calculated for each sampling date and species. In each analysis, the correlation coefficient (ρ) and the value of its significance level were calculated.

Group Analysis

Because canopy attributes change with the seasons, it is likely that individual trees will group together depending on the season in which measurements are made. Linear discriminant analysis was applied to each species using the *lda* function in the *vegan* package for R (Oksanen et al. 2020), a priori grouping sampling dates of Julian dates (Table 1) as a function of the variables describing the tree crowns (basal area, cover, and fractal dimension). The best number of clusters was determined by the *K*-means clustering method that minimises the within-group variation (*kmeans* function in the *stats* package for R; R Core Team 2020). Afterwards, a similarity analysis was made (Clarke 1993) to statistically verify the identity of the formed groups (*anosim* function in the *vegan* package for R; Oksanen et al. 2020). Finally, the Kruskal-Wallis and *post-hoc* de Mann-Whitney tests (*kruskal.test* in the *stats* package for R; Oksanen et al. 2020) were applied to identify the differences between cover and D between the groups identified in each species.

Results

Relationships of Tree Crown Fractal Dimension, Cover, and Size Values with Seasonal Changes in Weather Variables

The values of D were very similar in both oak species, ranging from 2.35 to 2.75 depending on the method used (Table 3; Fig. 1a, b, c). The highest fluctuation in D values that we observed corresponded to the transect variation method, which unlike the isotropic and transect variation methods, did not clearly show the pattern of change in D value (Fig. 1a, b, c).

Table 3 Minimum and maximum values of the fractal dimension (D) of *Quercus castanea* and *Q. Obtusata* crowns measured in composite images using three variability estimators

Estimator	Min value	Mean (\pm ee)	Quercus castanea [†]		Quercus obtusata ^{††}	
			Max value	Min value	Mean (\pm ee)	Max value
Square interval	2.324	2.448 (\pm 0.005)	2.619	2.317	2.443 (\pm 0.006)	2.626
Isotropic	2.429	2.601 (\pm 0.004)	2.752	2.370	2.595 (\pm 0.005)	2.750
Transect variation	2.346	2.554 (\pm 0.003)	2.657	2.307	2.541 (\pm 0.004)	2.644

NOTE: [†] $n=248$. ^{††} $n=192$. Figures in parentheses are standard errors

The highest D values that we observed occurred in the middle spring and in the early summer (Fig. 1a, b, c), when the mean monthly temperature is high ($\approx 20^\circ\text{C}$) and the accumulated precipitation is low (≈ 0.5 mm; Table 1). Between the two points of high D values, we observed a decrease occurring during the late spring, a time of the year when trees lose all of their foliage and the tree crowns become less complex (Fig. 1a, b, c).

The total variation of average crown cover we recorded ranged from 43 to $\sim 94.8\%$ in *Quercus castanea*, and from 34 to $\sim 93.6\%$ in *Q. obtusata*. The largest crown cover values occurred in the late summer and early fall, seasons with temperate temperatures and rainfall, the lowest values happening between early winter and early fall (Fig. 1d).

Variable Dynamics Analysis

Correlation Analysis of D and Morphometric Tree Attributes

A total of 56 spearman correlations between D and morphometric tree attributes for each species were obtained, most of them non-significant (Online resource 3). For *Q. obtusata* nine significant correlations were found, all negative, mostly of D values with crown cover. For *Q. castanea* only five correlations were significant, mainly of D values with crown cover and basal area.

Correlation Analysis of D and Environmental Variables

In *Quercus castanea*, the monthly mean temperature correlated negatively and statistically significantly with cover ($\rho = -0.7619$, P -value=0.0368), while in *Q. obtusata*, that correlation was negative but marginally non statistically significant ($\rho = -0.7143$, P -value=0.0576). In both species, we also observed a positive correlation between mean monthly temperature and D that was statistically significant in *Q. obtusata* ($\rho=0.7619$, P -value=0.037), but almost so in *Q. castanea* ($\rho=0.7143$, P -value=0.0576; Online resource 4).

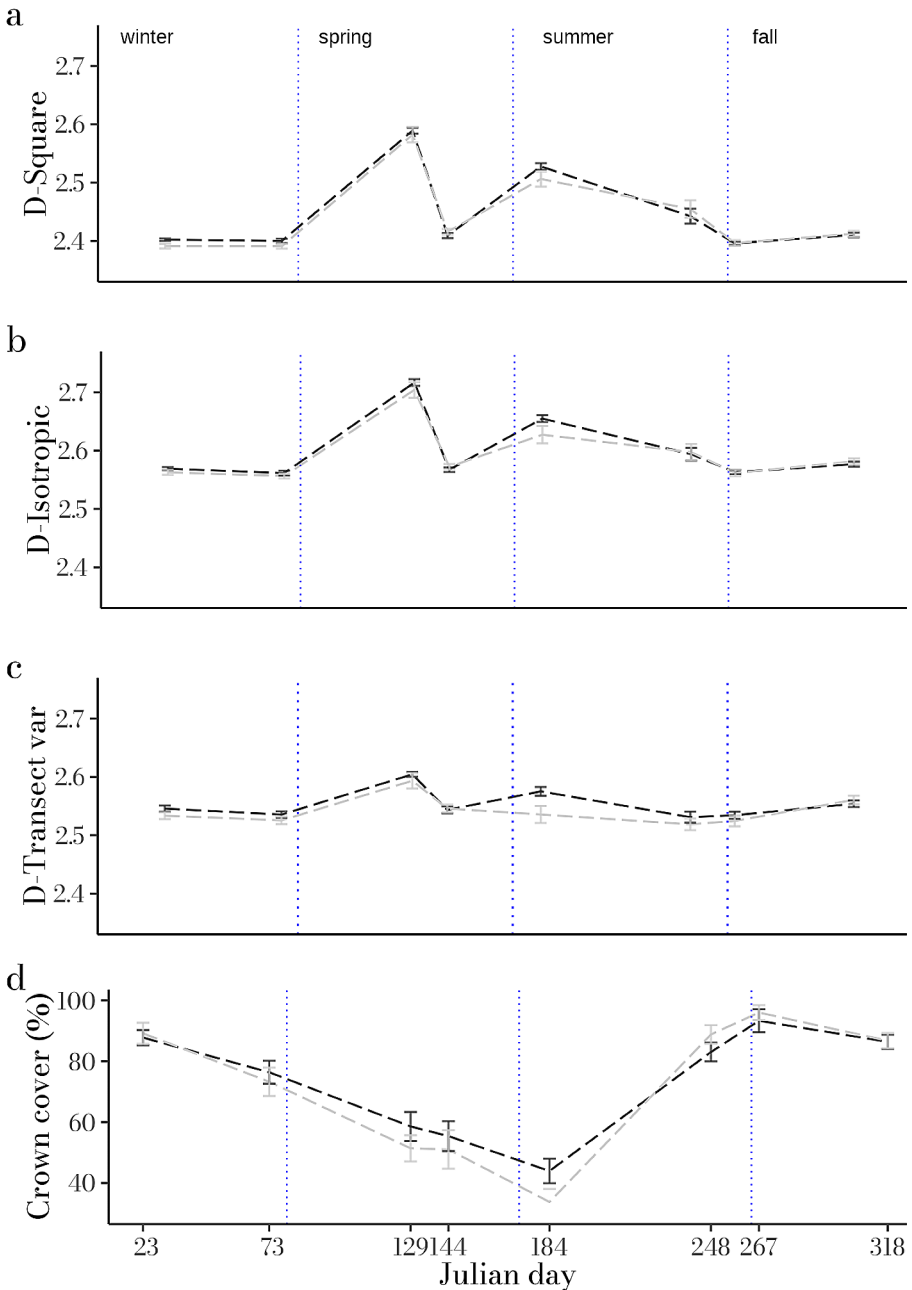


Fig. 1 Average values of fractal dimension (D) and tree crown cover of two species of *Quercus* in different measuring seasons throughout a Julian year and using three variation estimators of D
 NOTE: **a:** square increment (s). **b:** isotropic (i). **c:** transect variation (t). **d:** average percent tree crown cover. Dashed black line, *Quercus castanea* ($n=31$). Dashed grey line, *Quercus obtusata* ($n=24$). Dotted blue vertical lines indicate the beginning of the seasons

Group Analysis

In the group scatterplots for the three variable estimators that we applied, D and crown cover were in the first axis (LDA1), and D and basal area, in the second LDA2 (Fig. 2, Online resource 5). According to the results of the discriminant analysis, the sampling dates grouped differently to what was expected (Fig. 2). Our results of K -means clustering identified three groups in *Q. obtusata* for the three D estimators and in *Q. castanea* for the transect variation method, and only two groups for the square interval and isotropic methods in the latter species. The composition of sampling dates varied among K -means groups. The 3 and 5 Julian date samplings IDs grouped together in almost all scatterplots, while the rest of ID samplings grouped together in a second group (Fig. 2). The above-described grouping pattern was corroborated by the results of our χ^2 analysis for each date and species (Table 4).

Fractal dimension D was significantly different between all K -means groups for both species and the three D variation methods (Fig. 3). Crown cover differences between groups were also significant (Fig. 4), except for two cases (Fig. 4, d.f).

Discussion

In this work, we measured the fractal dimension (D) of deciduous tree crowns in natural conditions and for a long time period, as an innovative and simple approach to characterise forest canopy temporal dynamics.

Crown Cover Complexity Dynamics

The general pattern of tree crown temporal dynamics that we observed was characterised by two peaks with high complexity (high D values) and two valleys with low complexity (low D values) occurring throughout one Julian year (Fig. 1a, b, c). The valleys occurred in seasons with the highest and lowest tree crown cover and the crown complexity peaks, in the seasons with intermediate tree crown cover. While we observed similar patterns for the three variation estimator methods that we applied, the trends in tree cover temporal dynamics were clearer when we used the square increment method, for which we recommend its use for future studies.

Because we measured tree crown D values from an abstract 2D binary image, more voids appear in the image as the tree crown cover decreases, making it more complex (higher D values) (Arseniou & MacFarlane 2021). Reciprocally, when either all the foliage is lost or the tree crown is totally covered with leaves, the image becomes simpler (lower D values). Such a relationship between complexity and tree crown cover allowed us to observe a positive correlation between D and monthly mean temperature values, due to the latter weather variable determining leaf abscission; however, because D fluctuates differently from tree crown cover, the above relationship is not as clear in all sampling dates.

Based on the above-described results, we propose a model to aid in the understanding of deciduous tree crown temporal dynamics based on D values, which is graphically represented in Fig. 5. The model shows two crown complexity peaks and

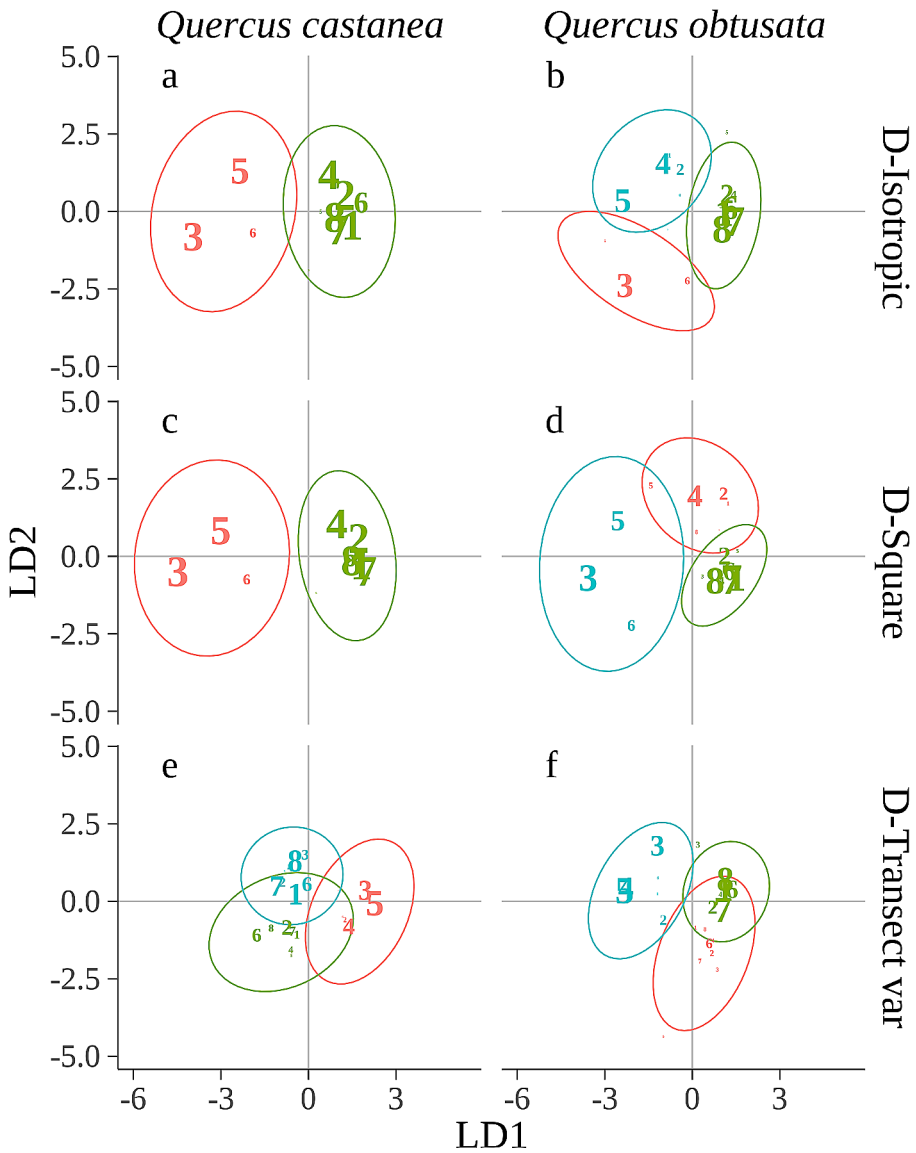


Fig. 2 First discriminant functions for two species of *Quercus*

NOTE: Left: *Quercus castanea* forming two groups (**a,c**) using the square increment (*D-Square*) and isotropic (*D-Isotropic*) methods, and three groups (**e**) using the transect variation (*D-Transect*) method ($R_{Sq}=0.1571$, $R_{Iso}=0.1741$, $R_{TV}=0.2269$, Significance=0.001). Right: *Q. obtusata* forming three groups (**b,d,f**) ($R_{Sq}=0.4886$, $R_{Iso}=0.5346$, $R_{TV}=0.4353$, Significance=0.001). Colours show the grouping suggested by the K-means analysis. Numbers correspond to the sampling date's ID (Table 1). Font size indicates the proportion of sampling dates classified within the group

Table 4 Proportion of sampling dates of *Quercus castanea* and *Q. obtusata* included within the linear discriminant analysis groups generated by the K-means method

	<i>Q. castanea</i>				<i>Q. obtusata</i>							
	ID	Orange (1)	Green (2)	χ^2	pvalue	ID	Orange (1)	Green (2)	Blue (3)	χ^2	pvalue	
Iso	1	0.00	100.00	31.000	0.0005	1	0.00	87.50	12.50	32.25	0.0005	
	2	0.00	100.00	31.000	0.0005	2	0.00	62.50	37.50	14.25	0.0030	
	3	93.55	6.45	23.516	0.0005	3	79.17	16.67	4.17	23.25	0.0005	
	4	0.00	100.00	31.000	0.0005	4	0.00	29.17	70.83	18.25	0.0005	
	5	87.10	12.90	17.065	0.0005	5	8.33	12.50	79.17	22.75	0.0005	
	6	32.26	67.74	3.903	0.081	6	25.00	75.00	0.00	21	0.0005	
	7	0.00	100.00	31.000	0.0005	7	0.00	100.00	0.00	48	0.0005	
	8	0.00	100.00	31.000	0.0005	8	0.00	91.67	8.33	37	0.0005	
Sq	ID	Orange (1)	Green (2)	χ^2	pvalue	ID	Orange (1)	Green (2)	Blue (3)	χ^2	pvalue	
	1	0.00	100.00	31.000	0.0005	1	12.50	87.50	0.00	32.25	0.0005	
	2	0.00	100.00	31.000	0.0005	2	41.67	58.33	0.00	13	0.0020	
	3	100.00	0.00	31.000	0.0005	3	0.00	12.50	87.50	32.25	0.0005	
	4	0.00	100.00	31.000	0.0005	4	70.83	29.17	0.00	18.25	0.0005	
	5	93.55	6.45	23.516	0.0005	5	20.83	12.50	66.67	12.25	0.0025	
	6	35.48	64.52	2.613	0.1524	6	4.17	58.33	37.50	10.75	0.0065	
	7	0.00	100.00	31.000	0.0005	7	0.00	100.00	0.00	48	0.0005	
Var	ID	Orange (1)	Green (2)	Blue (3)	χ^2	pvalue	ID	Orange (1)	Green (2)	Blue (3)	χ^2	pvalue
	1	0.00	29.03	70.97	23.677	0.0005	1	12.50	79.17	8.33	22.75	0.0005
	2	16.13	51.61	32.26	5.871	0.0655	2	20.83	45.83	33.33	2.25	0.3383
	3	64.52	0.00	35.48	19.419	0.0005	3	12.50	20.83	66.67	12.25	0.0030
	4	54.84	22.58	22.58	6.452	0.045	4	12.50	16.67	70.83	15.25	0.0005
	5	83.87	9.68	6.45	35.677	0.0005	5	8.33	4.17	87.50	31.75	0.0005
6	6.45	45.16	48.39	10.129	0.0065	6	33.33	58.33	8.33	9	0.0155	

Table 4 (continued)

	Q. castanea			Q. obtusata							
7	0.00	32.26	67.74	21.355	0.0005	7	16.67	83.33	0.00	28	0.0005
8	3.23	25.81	70.97	22.129	0.0005	8	12.50	79.17	8.33	22.75	0.0005

NOTE: ID: sampling julian date identification (Table 2). Orange (1), Green (2), and Blue (3); Groups and their identification numbers detected by the K-means method. Iso, Sq, and Var: Variation estimator methods applied in fractal dimension (D) calculation. For each sampling date, the results of the χ^2 (df=2) analyses are shown

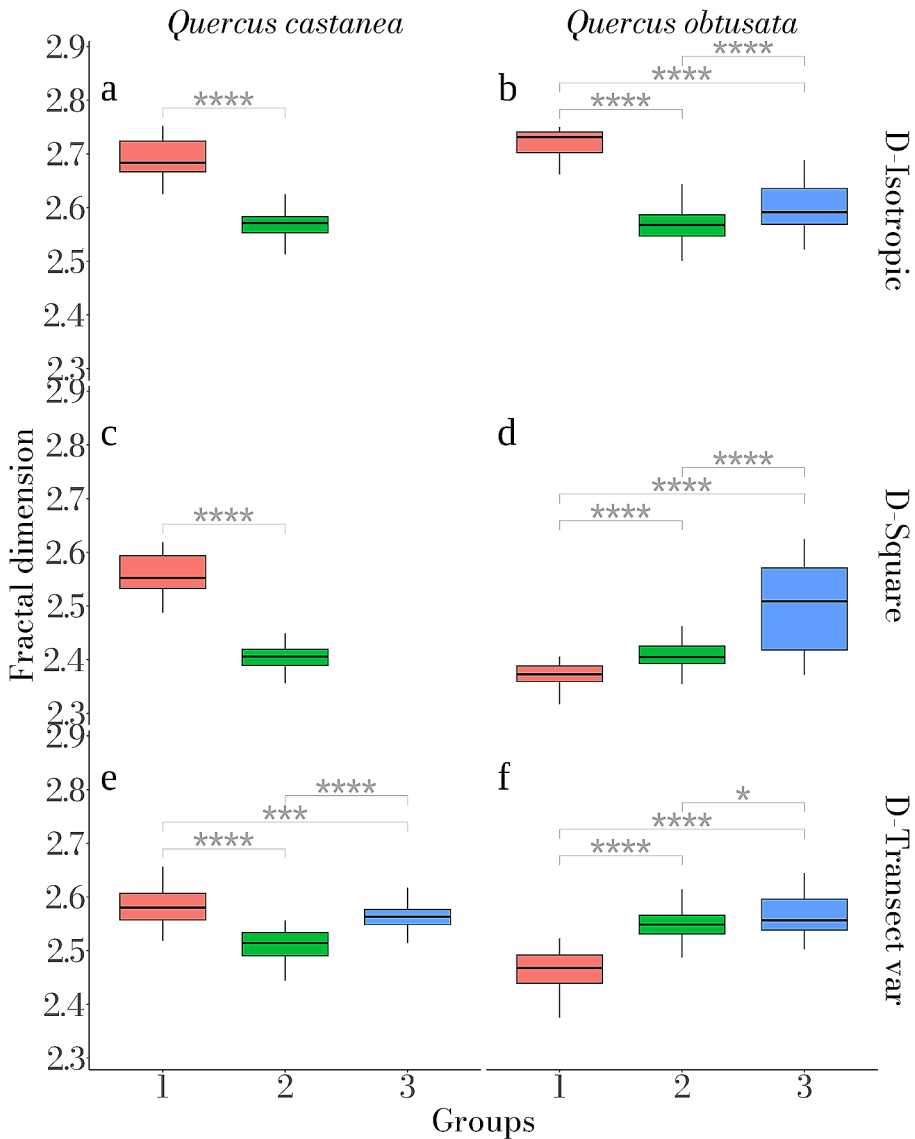


Fig. 3 Comparisons of fractal dimension by groups obtained with K-means analysis for three variation estimators of D

NOTE: D -Square: square increment. D -Isotropic: isotropic method. D -Transect: transect variation. **a,c,e**: *Quercus castanea*. **b,d,f**: *Quercus obtusata*. The results of the post hoc tests are shown above each group combination. *: p -value < 0.05. **: p -value < 0.01. ***: p -value < 0.001. *****: p -value < 0.0001

two valleys, the first peak will occur during leaf abscission and the second one, during new leaf development, in both cases, the crown cover having intermediate values. Between these two stages, two valleys will form, the first one of short duration and corresponding to the time in which trees are totally devoid of foliage (thus generating a less complex image), and a second stage—this one having the longest duration—in

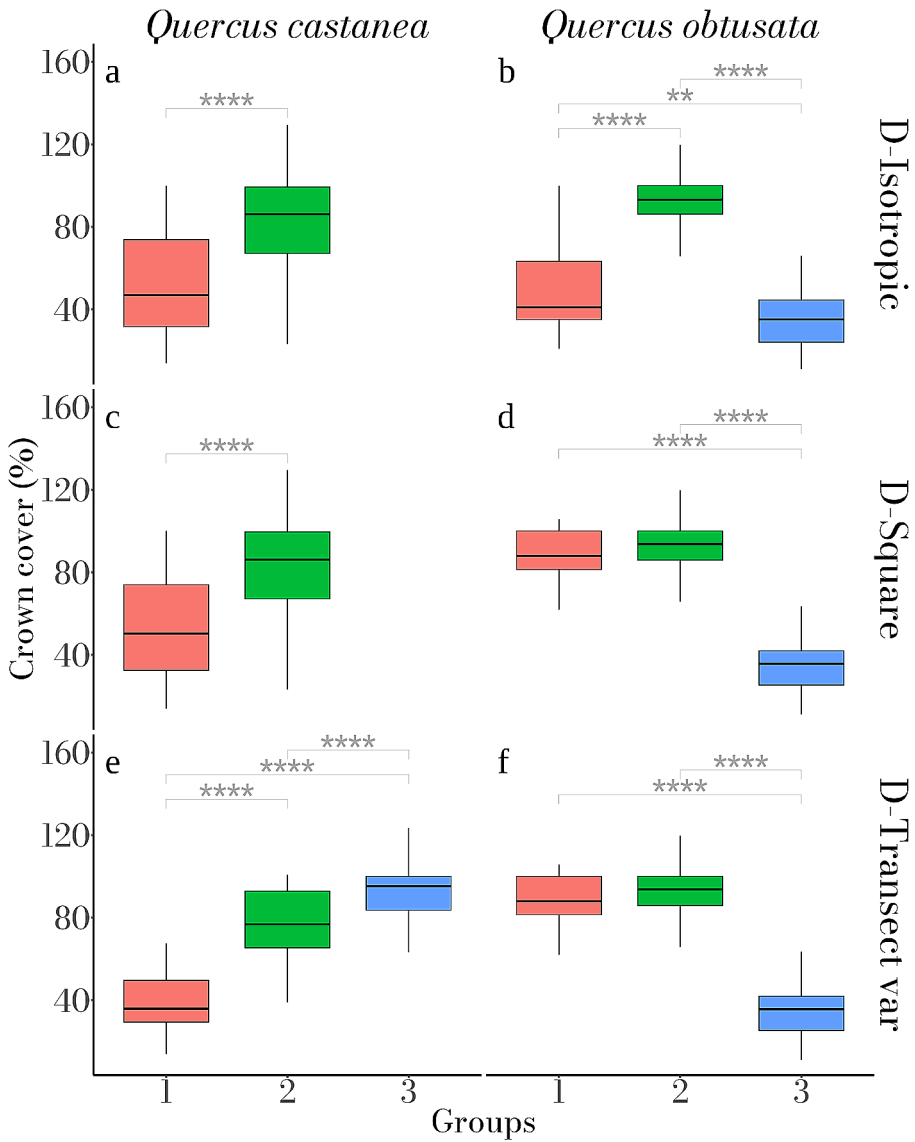


Fig. 4 Comparisons of percent tree crown cover by groups obtained with K-means analysis for three variation estimators of D

NOTE: D -Square: square increment. D -Isotropic: isotropic method. D -Transect: transect variation. **a,c,e**: *Quercus castanea*. **b,d,f**: *Quercus obtusata*. The results of the post hoc tests are shown above each group combination. *: p -value < 0.05. **: p -value < 0.01. ***: p -value < 0.001. ****: p -value < 0.0001

which leaves completely cover the tree crowns. During the latter stage, leaves change colour, a physiological process that we were unable to analyse in the black and white images that we used. As shown by the results of our analysis of crown cover, there will be some loss of leaves at the end of the second valley stage, but that loss will not be enough to drastically change the tree crown complexity values. In semi-deciduous

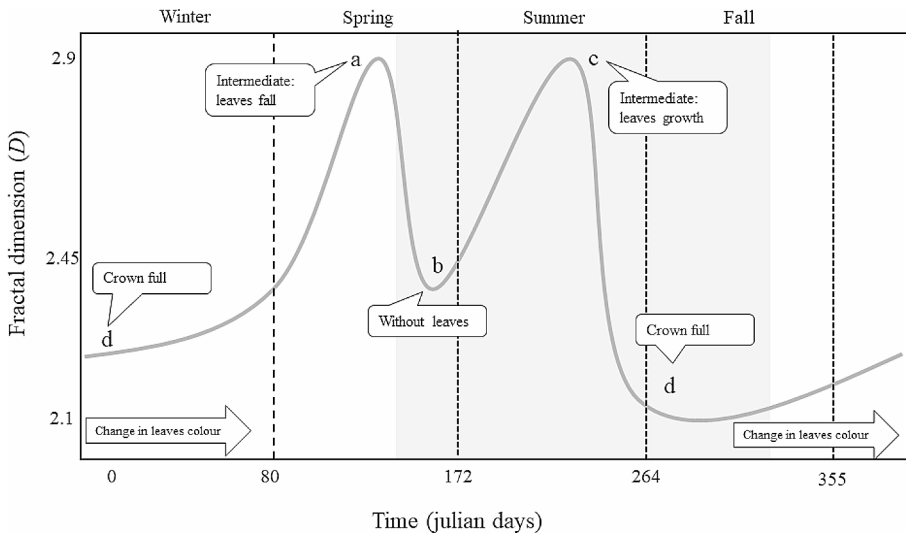


Fig. 5 Proposed model of deciduous tree crown temporal dynamics based on fractal dimension values (D)

NOTE: The x -axis corresponds to time in Julian days and the y -axis, to hypothetical D values. The approximate rainy period is represented by the grey shading. Dashed lines indicate the days in which season changes occur. The model assumes the occurrence of two peaks in D (a and c) corresponding to intermediate crown covers in which the images become more complex due to the presence of more voids. The valleys (b and d) represent the time in which the crown cover is completely devoid of foliage (b) and the valley d represents the time when the image shows a completely covered crown, in both cases the image becoming simpler. During the latter stage, physiological changes occur (leaf colour changes) that were undetected in the black and white (binary) images

tree species, the behaviour of the tree crown fractal dimension might vary, having only one valley (corresponding to intermediate crown cover stages) and one peak (corresponding to full tree crowns). In the case of evergreen tree species, according to the previous reports reviewed by Wang et al. (1992), it is possible that the tree crown fractal dimension reaches a nearly constant value, which would only change radically due to events that cause extreme modifications of the trees' architecture, caused by prunings, diseases, or strong winds (Kane et al. 2014).

Crown Cover Temporal Dynamics

The crown cover values that we observed represent the phenological curves of the studied oak species. The negative correlation of crown cover values with monthly mean temperature shows that this weather variable triggers leaf loss, as reported by Bello-González (1994) and Olvera-Vargas et al. (1997) in their analyses of oak phenology in temperate latitudes. We did not observe statistically significant relationships between crown cover dynamics and accumulated precipitation, which was perhaps due to the actual rainfall patterns in the study area differing from those recorded in the Morelia weather station. Vazquez et al. (1995) and Herrera-Marin (2013) recognized the link between precipitation and crown cover of *Q. castanea*, *Q. elliptica*, and *Q.*

insignis, because of which we might assume this relationship does occur in the oak species we studied, particularly so in *Q. castanea*.

Species Effect

The species here analyzed differ in anatomical attributes, like wood structure (Pérez-Olvera and Dávalos-Sotelo 2008), leaf area index and root depth (Meza-Rico et al. 2022). In this context, the coincidence of crown fractal dimensions values may reflect an environment-guided response in order to optimize light interception. Although Gričar et al. (2017) had considered species as a factor of tree crown variation, and Arseniou and MacFarlane (2021) recognized species as a crown complexity factor, we failed to find significant differences between crown cover and complexity in both studied species. Such discrepancy may have been due to the species we studied being congeneric, adapted to aridity and sharing environmental conditions, their close phylogenetic relationship making that the genetic control of their response thresholds to environmental variability be similar (Rousi & Pusenius 2005; Sanz-Pérez et al. 2010). The coexistence in the study site of the oak species we studied and their development in the same environmental conditions, might cause weather variables to become more relevant for determining the shaping of their crowns. Data of *Q. obtusata* were aggregated in three groups in each D variation method, while *Q. castanea* grouped mainly in two clusters. This may suggest that temporal and individual variation of *Q. obtusata* is consistently higher.

Tree Size Effects

Tree size measured as basal area—together with stem diameter and tree height—provided no information to understand tree crown temporal dynamics. Although other authors like Foroutan-pour et al. (2000) and Zhang et al. (2011) reported that plant age and size have effects on canopy complexity, we failed to observe such an effect, which we attributed to the individuals we sampled having similar size ranges and being adult trees, hence the sample lacking sufficient variability in size to show that relationship.

We expect that this work contributes to characterise tree crowns from a geometric and structural complexity approach. Our analysis allowed us to generate the first evidence of tree crown complexity being linked to crown cover and temperature changes. We suggest that future studies aiming at analysing the fractal dimension of deciduous tree species should involve a larger sampling effort during the season in which trees renew their foliage, which would allow refining, reinforcing, or rejecting the relationships between tree crown complexity and cover that we report here. Analyses of tree crown complexity could be coadjutant to researchers of vegetative phenology, light infiltration, and tree hydraulics, among other topics. Finally, the non-invasive technique we designed for this work allows using images to obtain data of temporal tree crown dynamics, which would make studies to be easily reproduced at a low cost.

Keeping in mind that fractal properties of natural objects occur in a limited scale range (Halley et al. 2004), fractal dimension is nevertheless a simple scale for mea-

suring complexity of systems and processes of apparently different nature, but sharing unifying attributes. For example, fractal analysis offers a theoretical frame to understand how size and metabolism of organisms are related (West et al. 1999), can be a proxy of physiological condition and of short-term adaptive response to stress (Wang et al. 2009), and can be used to test if such a variable attribute as tree crown architecture is heritable (Bailey et al. 2004).

Supplementary Information The online version contains supplementary material available at <https://doi.org/10.1007/s12229-023-09298-6>.

Acknowledgements We acknowledge the support of the late Dr. Pablo Alarcón Chaires, who facilitated our access to the Tsintani Renacer Voluntarily Conservation Area. The biologists Ignacio Palacios Ávila and Miguel A. Romero provided us with logistic support during samplings. Dr. Ellen Andresen made appropriate comments to improve early versions of this work. We acknowledge the Posgrado en Ciencias Biológicas, UNAM, and CONACYT (817856) for providing financial support for this work.

Author Contributions All authors contributed to the study conception and design. Material preparation, data collection and analyses were performed by Graciela Jiménez and Ernesto Vega. The first draft of the manuscript was written by Graciela Jiménez and all authors commented on previous versions of the manuscript. All authors read and approved the final manuscript.

Funding Graciela Jiménez has received research support from CONACYT 818756.

Declarations

Competing Interests The authors have no relevant financial or non-financial interests to disclose.

Compliance with Ethical Standards Research involving Human Participants and/or Animals is not applicable. Informed consent is not applicable.

Open Access This article is licensed under a Creative Commons Attribution 4.0 International License, which permits use, sharing, adaptation, distribution and reproduction in any medium or format, as long as you give appropriate credit to the original author(s) and the source, provide a link to the Creative Commons licence, and indicate if changes were made. The images or other third party material in this article are included in the article's Creative Commons licence, unless indicated otherwise in a credit line to the material. If material is not included in the article's Creative Commons licence and your intended use is not permitted by statutory regulation or exceeds the permitted use, you will need to obtain permission directly from the copyright holder. To view a copy of this licence, visit <http://creativecommons.org/licenses/by/4.0/>.

References

- Arseniou G., & MacFarlane, D.W. (2021). Fractal dimension of tree crowns explains species functional-trait responses to urban environments at different scales. *Ecological Applications*, e02297 31:1–13. <https://doi.org/10.1002/eap.2297>
- Backhous, D., & Nehl, D.B. (1999). Fractal geometry and soil wetness duration as tools for quantifying spatial and temporal heterogeneity of soil in plant pathology. *Australasian Plant Pathology*, 28:27–33. <https://doi.org/10.1071/AP99004>
- Bailey, J.K., Bangert, R.K., Schweitzer, J.A., Trotter, III R.T., Shuster, S.M., & Whitham, T.G. (2004). Fractal geometry is heritable in trees. *Evolution*, 58:2100–2102. <https://doi.org/10.1111/j.0014-3820.2004.tb00493.x>

- Bello-González, MAB. (1994). Fenología y Biología del desarrollo de cinco especies de *Quercus*, en Paracho y Uruapan, Michoacán. *Revista Mexicana de Ciencias Forestales*, 19: 3–40.
- Bréda, N., & Granier, A. (1996). Intra- and interannual variations of transpiration, leaf area index and radial growth of a sessile oak stand (*Quercus petraea*). *Annals of Forest Science*, 53:521–536.
- Bruno, O.M., de Oliveira, Plotze, R., Falvo, M., & de Castro, M. (2008). Fractal dimension applied to plant identification. *Information Sciences*, 178:2722–2733. <https://doi.org/10.1016/j.ins.2008.01.023>
- Burrough, P.A. (1981). Fractal dimensions of landscapes and other environmental data. *Nature*, 294: 240–242. <https://doi.org/10.1038/294240a0>
- Carlón-Allende T., & Mendoza, M.E. (2007). Análisis hidrometeorológico de las estaciones de la cuenca del lago de Cuitzeo. *Investigaciones Geográficas*, 63:56–76.
- Clarke, K.R. (1993). Non-parametric multivariate analysis of changes in community structure. *Australian Journal of Ecology*, 18, 117–143. <https://doi.org/10.1111/j.1442-9993.1993.tb00438.x>
- Constantine, W., & Percival, D. (2014). *Fractal: fractal time series modeling and analysis*. R package version, 2–0. https://cran.r-project.org/src/contrib/Archive/fractal/fractal_2.0-0.tar.gz
- R Core Team (2020). *R: A language and environment for statistical computing*. R Foundation for Statistical Computing, Vienna, Austria. URL <https://www.R-project.org/>
- Dirección de Medio Ambiente y Sustentabilidad de la Secretaría de Desarrollo Metropolitano (2018). *Informe Meteorológico Mensual*. [accessed 2022 Sep.302018]. http://www.morelia.gob.mx/pdfs/MICROSITIOS/MedioAmbiente/Calidad_Aire
- Dutilleul, P., Han L., Valladares, F., & Messier, C. (2015). Crown traits of coniferous trees and their relation to shade tolerance can differ with leaf type: a biophysical demonstration using computed tomography scanning data. *Frontiers in Plant Science*, 6:172. <https://doi.org/10.3389/fpls.2015.00172>
- Ehbrecht, M., Schall, P., Ammer, C., & Seidel, D. (2017). Quantifying stand structural complexity and its relationship with forest management, tree species diversity and microclimate. *Agricultural and Forest Meteorology*, 242:1–9. <https://doi.org/10.1016/j.agrformet.2017.04.012>
- Foroutan-pour, K., Dutilleul, P., & Smith, D.L. (2000). Effects of plant population density and intercropping with soybean on the fractal dimension of corn plant skeletal images. *Journal of Agronomy and Crop Science*, 184:89–100. <https://doi.org/10.1046/j.1439-037x.2000.00362.x>
- García, E. (1964). *Modificaciones al Sistema de Clasificación Climática de Köppen*. Instituto de Geografía, Universidad Nacional Autónoma de México, México. <http://www.publicaciones.igg.unam.mx/index.php/ig/catalog/view/83/82/251-1>
- Gneiting, T., Ševčíková, H., & Percival, D.B. (2012). Estimators of Fractal Dimension: Assessing the Roughness of Time Series and Spatial Data. *Statistical Science*, 27:247–277. <http://www.jstor.org/stable/41714797>
- Gričar, J., Lavrič, M., Ferlan, M., Vodnik, D., & Eler, K. (2017). Intra-annual leaf phenology, radial growth and structure of xylem and phloem in different tree parts of *Quercus pubescens*. *European Journal of Forest Research*, 136: 625–637. <https://doi.org/10.1007/s10342-017-1060-5>
- Halley, J.M., Hartley, S., Kallimanis, A.S., Kunin, W.E., Lennon, J.J., & Sgardelis, S.P. (2004). Uses and abuses of fractal methodology in ecology. *Ecology Letters*, 7: 254–271 <https://doi.org/10.1111/j.1461-0248.2004.00568.x>
- Hastings, H., & Sugihara, G. (1993). *Fractals. A user's guide for the natural sciences*. Oxford Science Publications. <https://ui.adsabs.harvard.edu/abs/1993fusb.book.....H/>
- Herrera-Marin, M. (2013). *Fenología de Quercus insignis M. Martens et Galeotti y Quercus xalapensis Bonpl. (FAGACEAE). en el jardín botánico de fundación Xochitla A. C* Dissertation, Universidad Nacional Autónoma de México.
- Ishii, H., & Asano, S. (2010). The role of crown architecture, leaf phenology and photosynthetic activity in promoting complementary use of light among coexisting species in temperate forests. *Ecological Research*, 25:715–722. <https://doi.org/10.1007/s11284-009-0668-4>
- Ivošević, B., Han, Y.G., Cho, Y., & Kwon, O. (2015). The use of conservation drones in ecology and wildlife research. *Journal of Ecology and Environment*, 38:113–118. <https://doi.org/10.5141/ecoenv.2015.012>
- Ivošević, B., Han, Y.G., & Kwon, O. (2017). Calculating coniferous tree coverage using unmanned aerial vehicle photogrammetry. *Journal of Ecology and Environment*, 41:1–8. <https://doi.org/10.1186/s41610-017-0029-0>
- Kane, B., Modarres-Sadeghi, Y., James, K.R., & Reiland, M. (2014). Effects of crown structure on the sway characteristics of large decurrent trees. *Trees*, 28:151–159. <https://doi.org/10.1007/s00468-013-0938-1>

- Kenkel, N.C., & Walker, D.J. (1996). Fractals in the biological sciences. *Coenoses*, 11(2): 77–100 URL: <https://www.jstor.org/stable/43461170>
- MacLeod, N., & Steart, D. (2015). Automated leaf physiognomic character identification from digital images. *Paleobiology*, 41:528–553. <https://doi.org/10.1017/pab.2015.13>
- Mandelbrot, B.B. (1982). *The fractal geometry of nature*. W. H. Freeman and Company, New York.
- Meza-Rico, L.M., Aguilar-Romero, R., Paz, H., Rodríguez-Correa, H., González-Rodríguez, A., Oyama, K., & Pineda-García, F. (2022). Functional differentiation among Mexican oak species is guided by the fast–slow continuum but above and belowground resource use strategies are weakly coordinated. *Trees*, 36:627–643. <https://doi.org/10.1007/s00468-021-02235-3>
- Musarella, C.M., Cano-Ortiz, A., Piñar-Fuentes, J.C., Navas-Ureña, J., Pinto-Gomes, C.J., Quinto-Canas, R., Cano, E., & Spampinato, G. (2018). Similarity analysis between species of the genus *Quercus* L (Fagaceae) in southern Italy based on the fractal dimension. *PhytoKeys*, 113:79–95. <https://doi.org/10.3897/phytokeys.113.30330>
- Nayak, S.R., Mishra, J., & Palai, G. (2019). Analysing roughness of surface through fractal dimension: A review. *Image and Vision Computing*, 89:21–34. <https://doi.org/10.1016/j.imavis.2019.06.015>
- Oancea, S. (2017). Fractal analysis of the modifications induced on tomato plants by heavy metals. *Stiinta agricola*, 1:36–38.
- Oksanen, J., Blanchet, F.G., Friendly, M., Kindt, R., Legendre, P., McGlenn, D., Minchin, P.R., O'Hara, R.B., Simpson, G.L., Solymos, P., Stevens, M.H.H., Szoecs, E., Wagner, H. (2020). *vegan: Community Ecology Package*. R package version 2.5-7. <https://CRAN.R-project.org/package=vegan>
- Olvera-Vargas, M., Figueroa-Rangel, B.L., Moreno-Gómez, S., & Solís-Magallanes, A. (1997). Resultados preliminares de la fenología de cuatro especies de encino en Cerro Grande, Reserva de la Biosfera Sierra de Manantlán. *Biotam*, 9:7–18.
- Osawa, A. (1995). Inverse relationship of crown fractal dimension to self-thinning exponent of tree populations: a hypothesis. *Canadian Journal of Forest Research*, 25:1608–1617. <https://doi.org/10.1139/x95-175>
- Öztürk, M. (2016). Complete intra-annual cycle of leaf area index in a *Platanus orientalis* L. stand. *Plant Biosystems*, 150:1296–1305. <https://doi.org/10.1080/11263504.2015.1054446>
- Palmer, M.W. (1988). Fractal geometry: a tool for describing spatial patterns of plant Communities. *Veg- etatio*, 75: 91–102. <https://doi.org/10.1007/BF00044631>
- Pangga, I.B., Hanan, J., & Chakraborty, S. (2013). Climate change impacts on plant canopy architecture: implications for pest and pathogen management. *European Journal of Plant Pathology*, 135: 595–610. <https://doi.org/10.1007/s10658-012-0118-y>
- Pentland, A.P. (1984). Fractal-based description of natural scenes. *IEEE PAMI*, 6: 661–674. <https://doi.org/10.1109/TPAMI.1984.4767591>
- Pérez-Olvera, C., & Dávalos-Sotelo, R. (2008). Some anatomical and technological characteristics of 24 *Quercus* wood species (oaks) of Mexico. *Madera y Bosques*, 14(3):43–80
- Romero-Rangel, S., Rojas-Zenteno, E.C., & Rubio-Licona, L.E. (2014). Fagaceae. *Flora del Bajío y de regiones adyacentes*, 181:1-169.
- Rousi, M., & Pusenius, J. (2005). Variations in phenology and growth of European white birch (*Betula pendula*) clones. *Tree Physiology*, 25: 201–210. <https://doi.org/10.1093/treephys/25.2.201>
- Sala, F., Dăţcu, A.D., & Rujescu, C. (2020). Fractal dimension and causality relationships with foliar parameters: case study at *Alnus glutinosa* (L.) Gaertn. *Annals of West University of Timișoara. Series of Biology*, vol. 23:73–82.
- Sanz-Pérez, V., & Castro-Díez, P. (2010). Summer water stress and shade alter bud size and budburst date in three Mediterranean *Quercus* species. *Trees*, 24: 89–97. <https://doi.org/10.1007/s00468-009-0381-5>
- Seidel, D. (2018). A holistic approach to determine tree structural complexity based on laser scanning data and fractal analysis. *Ecology and Evolution*, 8: 128–134. <https://doi.org/10.1002/ece3.3661>
- Seidel, D., Ehbrecht, M., Dorji, Y., Jambay, J., Ammer, C., & Annighöfer, P. (2019). Identifying architectural characteristics that determine tree structural complexity. *Trees*, 33: 911–919. <https://doi.org/10.1007/s00468-019-01827-4>
- Sugihara, G., May, & R.M. (1990). Applications of fractals in ecology. *Trends in Ecology and Evolution*, 5(3): 79–86. [https://doi.org/10.1016/0169-5347\(90\)90235-6](https://doi.org/10.1016/0169-5347(90)90235-6)
- Vázquez, J.A., Cuevas, R., Cochrane, T.S., Iltis, H.H., Santana, F.J., Guzman, L. (1995). *Flora de Manantlán*. BRIT Press.
- Wang, J., Ives, N.E., & Lechowicz, M.J. (1992). The relation of foliar phenology to xylem embolism in trees. *Functional Ecology*, 6:469–475. <https://doi.org/10.2307/2389285>

- Wang, H., Siopongco, J., Wade, L.J., & Yamauchi, A. (2009). Fractal analysis on root systems of rice plants in response to drought stress. *Environmental and Experimental Botany*, 65 (2009) 338–344. <https://doi.org/10.1016/j.envexpbot.2008.10.002>
- West, G.B., Brown, J.H., & Enquist, B.J. (1999). The fourth dimension of life: fractal geometry and allometric scaling of organisms. *Science*, 284 (4), 1677:1679. <https://doi.org/10.1126/science.284.5420.1677>
- Xu, Y., Du, C., Huang, G., Li, Z., Xu, X., Zheng, J., & Wu, C. (2020). Morphological characteristics of tree crowns of *Cunninghamia lanceolata* var. Luotian. *Journal of Forestry Research*, 31: 837–856. <https://doi.org/10.1007/s11676-019-00901-4>
- Yang, X.C., & Hwa, C.M. (2008). Genetic modification of plant architecture and variety improvement in rice. *Heredity*, 101: 396–404. <https://doi.org/10.1038/hdy.2008.90>
- Yang, X.D., Yan, E.R., Chang, S.X., Da, L.J., & Wang, X.H. (2015). Tree architecture varies with forest succession in evergreen broad-leaved forests in Eastern China. *Trees*, 29: 43–57. <https://doi.org/10.1007/s00468-014-1054-6>
- Zeide, B., & Pfeifer, P. (1991). A method for estimation of fractal dimension of tree crowns. *Forest Science*, 37: 1253–1265. <https://doi.org/10.1093/forestscience/37.5.1253>
- Zhang, S., Li, B., Liu, Y., Zhang, L., Wang, Z., & Han, M. (2011). Fractal characteristics of two-dimensional images of 'Fuji' apple trees trained to two tree configurations after their winter pruning. *Scientia Horticulturae*, 130: 102–108. <https://doi.org/10.1016/j.scienta.2011.06.018>
- Zhu, J., Wang, X., Chen, J., Huang, H., & Yang, X. (2014). Estimating fractal dimensions of tree crowns in 3-D space based on structural relationships. *The Forestry Chronicle*, 90: 177–183. <https://doi.org/10.5558/tfc2014-035>

Publisher's Note Springer Nature remains neutral with regard to jurisdictional claims in published maps and institutional affiliations.